SPACE SCIENCES LABORATORY

N72-22807

The Spectra of Ten Galactic X-ray Sources in the Southern Sky

Ray Cruddace, Stuart Bowyer, Michael Lampton, John Mack, and Bruce Margon

Department of Astronomy and Space Sciences Laboratory, University of California, Berkeley

October 1971

CASE FILE COPY

This work was supported by NASA Grant NGR 05-003-278.

Space Sciences Laboratory Series 12 Issue 74

UNIVERSITY OF CALIFORNIA, BERKELEY

Space Sciences Laboratory
University of California
Berkeley, California 94720

THE SPECTRA OF TEN GALACTIC X-RAY SOURCES IN THE SOUTHERN SKY

Ray Cruddace, Stuart Bowyer, Michael Lampton,
John Mack, and Bruce Margon

Department of Astronomy and Space Sciences Laboratory,
University of California, Berkeley

October 1971

This work was supported by NASA Grant NGR 05-003-278
and is prepared for submittal to *The Astrophysical Journal*.

Space Sciences Laboratory Series 12 Issue 74

THE SPECTRA OF TEN GALACTIC X-RAY SOURCES IN THE SOUTHERN SKY

RAY CRUDDACE, STUART BOWYER, MICHAEL LAMPTON,
JOHN MACK,* AND BRUCE MARGON

Department of Astronomy and Space Sciences Laboratory,
University of California, Berkeley

ABSTRACT

Data on ten galactic X-ray sources located between $\ell_{II} = 320°$ and $\ell_{II} = 20°$ were obtained during a rocket flight from Brazil in June 1969. Detailed spectra of these sources have been compared with bremsstrahlung, black body, and power law models, each including interstellar absorption. Six of the sources were fitted well by one or more of these models. In only one case were the data sufficient to distinguish the best model. Three of the sources were not fitted by any of the models, which suggests that more complex emission mechanisms are applicable. A comparison of our results with those of previous investigations provides evidence that five of the sources vary in intensity by a factor of 2 or more, and that three have variable spectra. New or substantially improved positions have been derived for four of the sources observed.

---

* Part of this paper submitted to Catholic University, Washington, D.C., in partial fulfillment of the requirements for the Ph.D. degree. Present address: Department of Physics, University of Houston, Houston, Texas 77004.

I. INTRODUCTION

The results to be described were obtained during the flight of an Aerobee 150 rocket, launched at $21^h\ 52^m$ U.T. on June 14, 1969, from Natal in Brazil. The early part of the flight was devoted to extragalactic observations (Bowyer *et al.* 1970, Lampton *et al.* 1971), after which the rocket was oriented to view the galactic disc in a rolling scan. The scan started at $\ell_{II} = 20°$ and proceeded at 6.3°/sec toward the galactic center. As the main purpose was to observe sources in the Scorpius-Norma-Lupus region, at $\ell_{II} = 5.8°$ the roll rate was reduced to 1°/sec, and the scan proceeded at this rate for the rest of the flight.

Galactic X-ray sources were observed by two proportional counters, both with P-10 gas at a pressure of about 1 atm and Mylar windows with a thickness of about 3.8 μ. The two X-ray collimators were made of aluminum honeycomb, and provided a small circular field of view (1.6° FWHM) for one detector and a slot (3° × 12° FWHM) inclined at 60° to the scan track for the other. Pulse-height analyzers were used to measure the photon energy distribution between 0.07 and 10 keV. The design and operation of the two detectors have been discussed in more detail by Bowyer *et al.* (1970).

In this paper we shall present the spectra of ten galactic sources observed during the flight, a comparison of the strengths and spectra of the sources with the results of other workers, and some new information on the positions of certain sources, particularly those in the Norma-Lupus region of the sky. When comparing our results with those obtained in other flights, we shall use the code in Table 1 to avoid frequent repetition of references.

II. LOCATION OF THE SOURCES

A map of the scan track of the detectors in galactic coordinates is shown in Figure 1. The galactic X-ray sources observed during the flight are identified as follows:

a. Black rectangles, which are the error boxes of newly discovered sources or sources for which this flight has provided improved positions.

b. Shaded circles and dots, which are the error circles of sources whose positions were defined by the MIT rocket surveys (Bradt *et al.* 1971).

c. Sco XR-7, the error box of this source being that defined in the LRL catalogue (Seward 1970).

The scan track has been defined using the roll rate of the payload, the known positions of certain X-ray sources, and sightings of sources by both detectors. A review of the rocket attitude control system established the roll rate with an accuracy of 1%, which permitted unambiguous identification of sources located precisely during three MIT flights (Bradt *et al.* 1971). These sources (GX 17+2, GX 13+1, GX 9+1, GX 5-1, GX 3+1, GX 349+2, and GX 340+0) were placed by MIT inside error circles whose radii never exceeded 17 minutes.

The change to a roll rate of 1°/sec occurred during the transit of GX 5-1. During this maneuver the roll axis started to precess slightly, causing the latitude of the scan track to rise slowly as GX 349+2 approached the field of view. As the MIT surveys did not extend beyond 340°, we have used transits of Cen XR-2 in both detectors

at a longitude of 308° ±1° to fix this part of the scan track. The position error circles of Cen XR-2 measured in four rocket flights (Rao *et al.* 1969, Chodil *et al.* 1967, Cooke *et al.* 1967, Harries *et al.* 1967) make it highly probable that the latitude of the source lies between +3° and -3°. Therefore we have traced the nominal scan track through ℓ_{II} = 308°, b_{II} = 0°, acknowledging latitude error limits of +3° and -2°. The negative limit is restricted by the sightings of GX 349+2 and GX 340+0 in both detectors.

The source GX -2.5 was located in longitude to ±0.15° during a rocket flight (ASE) and matches the source O1 seen by UHURU, for which no latitude yet has been reported. These sightings both may have included two sources at similar longitudes, as the longitude 357.5° passes through the position error circle of the source GX 358-8 (MIT III), shown in Figure 1 with a radius of 35 minutes, and of the source M1 detected at energies between 20 and 40 keV during a balloon flight (Lewin *et al.* 1969). The position error circle of M1 is centered at ℓ_{II} = 357°, b_{II} = 2°, and has a radius of 3°. This interpretation has been verified by the results of our flight, which located the source GX 357+2.5 within a 0.5° × 0.5° error box and which observed GX 358-8 at the edge of the field of the 3° × 12° collimator.

Until recently, the positions of sources at longitudes less than 340° were ill-defined. Norma XR-1, Norma XR-2, and Lupus XR-1 were reported first in 1967 (NRL II), but although these sources have been detected in several rocket flights (LRL I and II, UL I and II, PRL), none of the positions reported had sufficient accuracy to dispute those established in the first findings. Accordingly, between longitudes of

340 and 320° the LRL catalogue of X-ray sources (Seward 1970) shows the three NRL positions with error circles of radius 1.5°. These positions are shown in Figure 1.

However, UHURU discovered four sources between longitudes of 340 and 320° whose longitudes did not match these NRL positions well. The sources we have found and labelled GX 337+0 and GX 321-0.5 have the same longitudes as the sources J1 and G1 identified by UHURU. The source GX 327+4.5 was seen only by the detector with the wide field of view. In order to deduce its latitude, we have identified it with the source H1 seen by UHURU. The resulting latitude, 4.5 ± 1.5°, places it near the edge of the UHURU collimator field. This would tend to produce a low count-rate in the UHURU detector and we note that the count-rate from H1 was one-sixth that from G1. We have identified tentatively the sources GX 321-0.5 and GX 327+4.5 with Norma XR-2 and Lupus XR-1, respectively.

The count histogram of the detector with the 3° × 12° field of view showed a prominent peak between the transits of GX 5-1 and GX 3+1, giving the highest count-rate measured during the flight. The source of this peak lies in the long slot shown in Figure 1, and the only candidates we have found are Ophiuchus XR-2 (Seward 1970) and the variable source GX 1+4 discovered during an MIT balloon flight (Lewin *et al.* 1971). We shall not consider the source further, as the uncertainty in its position and the confusion with other sources preclude any determination of its intensity or spectrum.

The positions and error box dimensions of those sources for which this flight provided new locations are given in Table 2. The uncertainties in ℓ_{II} and b_{II} are the R.M.S. dispersions in position, based on possible errors in the roll rate and the source identification on the count histogram.

III. ANALYSIS OF THE SOURCES

Where a source has not been isolated sufficiently for the purpose of spectral analysis by either detector, the analysis of the source has been confined to an estimate of the energy flux at the earth in the 1 to 10 keV energy band. This has been done by decomposing the count histogram produced by confused sources, using the source locations defined in Figure 1.

The pulse height spectrum for each source well-isolated in either detector was compared with that expected from three model distributions of the photon flux, I:

Bremsstrahlung model: $$I = C \exp(-N_H \sigma)\, \bar{g} \exp(-E/kT)/[E(kT)^{\frac{1}{2}}] \qquad (1)$$

Power law model: $$I = C \exp(-N_H \sigma)\, E^{-n} \qquad (2)$$

Black body model: $$I = C \exp(-N_H \sigma) \frac{E^2}{\exp \frac{E}{kT} - 1}, \qquad (3)$$

where E and kT are in keV, and I is in photons cm^{-2} sec^{-1} keV^{-1}.

In these expressions N_H is the column density of hydrogen in the line of sight, σ is the X-ray photoabsorption cross section of the interstellar medium (Brown and Gould 1970), C is a free parameter representing the source intensity, and $\bar{g}$ is the Gaunt factor derived from the Born approximation for free-free collisions in a thermal plasma (Greene 1959):

$$\bar{g} = \frac{(3)^{\frac{1}{2}}}{\pi} \cdot \exp(E/2kT)\, K_o(E/2kT) . \qquad (4)$$

The analysis of a source proceeded by adjusting C, N_H, and n or T, and seeking the best fit of theory with observations by a minimum χ^2 technique. A grid (N_H, n) or N_H, T) was specified for each model, and the spectrum was evaluated at each grid point at 0.1-keV intervals between 0.1 and 11.0 keV, assuming C = 1. Each spectrum then was multiplied by the detector efficiency and convolved with a Poisson energy resolution kernel:

$$S(E,Y) = \frac{e^{-E/Q}}{Q} \cdot \frac{(E/Q)^{Y/Q}}{\Gamma(Y/Q + 1)} \quad . \tag{5}$$

This kernel describes the distribution of pulse heights, Y, originating from X-rays of energy E, where Q is the mean ionization energy per primary electron. We have measured the detector resolution at 5.9 keV to be 20% (FWHM), which yields the value 43 eV for Q.

Following these operations, the spectrum was integrated across each pulse height band K, to give an unnormalized channel spectrum F(K). The model accumulations M(K) = AtCF(K) + tB(K) were then calculated from the exposure time t, detector area A, and background count rate B(K). Finally, these numbers were compared with the data accumulation D(K) by calculating the quantity

$$\chi^2 = \sum_K \frac{[M(K) - D(K)]^2}{M(K)} \quad . \tag{6}$$

At each grid point a minimum of χ^2 was found by varying C, producing a two-dimensional map with coordinates N_H and n or T.

From such a map we obtained the values of N_H, n or T for the best fitting spectrum, the confidence in this result expressed by the minimum value of χ^2, and a tolerance contour for each model. Outside such a contour, the confidence at each grid point falls below $e^{-\frac{1}{2}}$ or 60.6% of the confidence at the best-fit point. This contour is analogous to the standard deviation of a Gaussian variate.

The χ^2 statistic is a measure of both systematic errors in the models and random count rate fluctuations in the data. The correct model and choice of parameter cause the probability of obtaining a given value of χ^2 to be given by the usual χ^2 distribution. An incorrect choice of model parameter will introduce systematic errors into the sum and on the average will increase χ^2. We shall measure the goodness of fit quantitatively by ranking the observed statistic χ^2 within the theoretical distribution by means of its confidence: $\int_{\chi^2_{obs}}^{\infty} P(\chi^2)\, d\,\chi^2$. On the average, this quantity will be 50% for perfectly fitting models. Using an established criterion (see, for example, Evans 1955) we shall regard a fit as satisfactory if its confidence falls between 10 and 90%.

In the initial analysis of each source, all 16 energy channels were used, but after careful allowance had been made for the efficiency and photon energy dispersion of the detectors in the soft channels, it was found that in most cases there were insufficient counts in the first three channels to give useful accuracy. In only two cases (namely, GX 340+6 and GX 357+2.5) did we use count-rates in the third channel (0.7-0.96 keV), because the obscuration of these sources by galactic hydrogen was less than that of other sources seen during the flight, and consequently, more counts were registered between 0.7 and 0.96 keV.

The energy fluxes observed from galactic X-ray sources during the flight are summarized in Table 3, where they are compared with the results of previous flights dating back to 1964. Corrections have been applied which refer all energy fluxes to the 1 to 10 keV band. Although caution should be used in comparing results obtained by different groups, the data presented in Table 3 suggest that the X-ray emissions from several of these sources are variable.

The early NRL flights used wide-field collimators (8° FWHM), so that the sources reported may have been confused. This may explain why, in a majority of cases, the flux intensities measured in these flights were larger than those made in subsequent flights. However, two notable exceptions are GX 321-0.5 and GX 327+4.5, which were far weaker during the NRL II flight than in two subsequent flights (LRL I and UCB). These two sources were seen also by UHURU in December 1970, and a study of the results shows that their count-rates, corrected for position in the collimator field, were less than our results by factors of 6 and 20, respectively. Cooke and Pounds (1971) reported a change in the energy flux from Lupus XR-1 (GX 327+4.5) between two rocket flights by at least an order of magnitude, but found little change in Norma XR-2 (GX 321-0.5). We interpret the sum of this evidence as showing that GX 321-0.5 and GX 327+4.5 are variable X-ray sources.

Following the early NRL flights, collimators with narrow fields of view were flown. As a result, sources were located and isolated with greater accuracy. Table 3 summarizes the results from six such flights, extending from 1966 to 1969. Some of the differences in intensities reported by these groups may be due to instrument errors, and therefore, it is safe to suspect of variability only those sources showing large

variations. Adopting intensity variations greater than a factor 2 as a criterion, we identify GX 349+2 and GX 13+1 as variable X-ray sources and confirm the recent UHURU result that GX 17+2 varies.

We have examined also our data from the sources listed in Table 3 for possible short time-scale, periodic intensity fluctuations, employing techniques outlined by Lampton *et al.* (1970). Although the short observing time for each source and the 128-ms telemetry sample period limited the effectiveness of this search, Circinus XR-1 (GX 321-0.5) was identified as a pulsating source with a period of 685 ±30 milliseconds (Margon *et al.* 1971a). No other sources were observed to pulse.

The results of the spectral analysis of the sources observed in this flight are summarized in Table 4, in which we present for each source the parameters of the best fitting spectrum for each of the three models. The spectra of these sources are shown in Figures 2 through 11, in which we have plotted the measured photon flux incident upon our detectors, the best fitting model spectrum, and where available, the results obtained from other rocket flights. Below each graph appear the tolerance contours for those models receiving confidences between 10 and 90%.

The spectrum of GX 321-0.5 has been measured in four rocket flights with the results shown in Figure 2, among which there is little agreement. Our results are fitted best by a black body spectrum, although bremsstrahlung emission is not ruled out. The results of other flights have been fitted with both bremsstrahlung and power law spectra, but the data obtained on this flight are not compatible with a power law model. The PRL and LRL II measurements diverge from our spectrum above 5 keV and yield a flux five times larger at 10 keV. The UL I results likewise yield a harder spectrum, but with a lower intensity. However, the new

positions found for GX 321-0.5 and GX 327+4.5 raise the possibility that during analysis of the University of Leicester flights, these two sources were mis-identified, and that the UL I spectrum shown in Figure 2 is that of GX 327+4.5. This suspicion is strengthened by the marked resemblance of this spectrum to our spectrum of GX 327+4.5. Even if the Leicester results are set aside for these reasons, we conclude nonetheless from the difference among the LRL, UCB, and PRL results that GX 321-0.5 has a variable spectrum.

The spectrum of GX 327+4.5 (Fig. 3) was fitted with about equal likelihood to a bremsstrahlung and to a power law spectrum. Despite the variability of this source, our spectrum is close to the LRL I spectrum measured in 1967. The spectrum of GX 337+0 (Fig. 4) was fitted with poor confidence by all three models, which may be due to source confusion, as UHURU discovered a weak source (I1) nearby at $\ell = 335°$. We were unable to resolve I1 in either collimator. The source GX 340+0 has been the subject of a separate paper (Margon *et al.* 1971b), as the results were of especial interest. The data (Fig. 5) were fitted to a black body spectrum with a confidence of 25%, which was significantly better than the confidences obtained with the other models.

Spectra of two sources observed in the Scorpius region (GX 349+2 and GX 340+6) are shown in Figures 6 and 7. The sources GX 340+6 and Sco XR-7 were confused by the detector with the 3° × 12° field of view. However, after decomposing the count histogram from this detector we estimated that GX 340+6 was the stronger by about a factor 6, which is reasonably in agreement with the factor 4 deduced from the LRL catalogue (Seward 1970). Therefore, approximately 80% of the counts were caused by the stronger source, so that the spectrum shown in Figure 6 is mainly that of GX 340+6.

It was fitted best with a confidence of 10% to a bremsstrahlung model. The low confidence and large tolerance contour of this source are almost certainly the result of source confusion.

The measurements of GX 349+2 proved remarkably difficult to fit with all three models, despite the fact that the source was well isolated and produced a high count-rate. The greatest confidence was of order 10^{-4}%. Spectra measured in 1965 (LMSC) and 1968 (LRL II) were significantly harder than the UCB spectrum, from which we conclude that its spectrum is variable.

Between longitudes of 350° and 20°, sources were confused by the detector with the 3° × 12° field of view, and spectra could be obtained only from four sources seen by the narrow-field detector. The spectra of GX 357+2.5, GX 3+1, GX 9+1, and GX 17+2 are shown in Figures 8 through 11. Due to the lower number of counts recorded by the detector with the narrow field of view, the results are subject to larger statistical uncertainties than those shown in the previous figures. Therefore the tolerance contours are larger, despite the respectable confidence achieved in fitting some of the measurements. The results of other measurements of the spectra of GX 9+1 and GX 17+2 are shown also in Figures 10 and 11, respectively. A wide scatter is obvious in the data reported for GX 17+2, which confirms the recent UHURU result that the spectrum of this source varies. The temperature of the spectrum we obtained from our flight is the lowest recorded, less than one-fifth the highest temperature measured by UHURU.

In Table 5 we list those sources which appear to have variable spectra, based on comparisons of our spectral analyses with those made by other groups. We have chosen the temperature of the best fitting

bremsstrahlung spectrum as a parameter for comparison, because of its widespread use among various experimental groups. Our criterion of spectrum variability is a scatter in the reported temperatures greater than a factor 2.

IV. DISCUSSION AND CONCLUSIONS

A comparison of our results for ten X-ray sources with those obtained by other groups shows that a significant number of these sources are variable in both intensity and spectrum over periods no greater than 1 year. Of those sources showing intensity variations, GX 321-0.5, GX 327+4.5, GX 349+2, GX 13+1, and GX 17+2 vary by factors greater than 2, and GX 327+4.5 may vary by a factor of 5 or more. Of those sources showing spectral variations, the temperatures of two sources, GX 321-0.5 and GX 349+2, vary by at least a factor 2, and the temperature of GX 17+2 may vary by a factor as great as 5.

Of the ten source spectra obtained from this flight, six are fitted with high confidence by one or more of the emission models we employed. The confidences of the fits of these six are not distributed randomly about 50%, which indicates that even for these sources the models employed are not perfect, or that there are some systematic experimental errors. Nonetheless, the distribution of confidences is sufficiently good to indicate that both our method of analysis and the models employed were adequate for the data at hand.

Discrimination between thermal and nonthermal models requires particularly sensitive measurements at the higher photon energies. The detectors used in this flight were relatively insensitive at these energies, and

consequently, we were unable to distinguish thermal and power law models, except in the case of GX 321-0.5, for which the power law model provided a poor fit. Flux differences between black body and highly absorbed bremsstrahlung models are not great and in order to distinguish between these models, X-ray instruments must exhibit a high sensitivity over a large range of energies. Only in the case of GX 340+0 can we choose between these models, and this source has been discussed in detail elsewhere (Margon *et al.* 1971b). However, the fact that three of the sources reported here were fitted best by black body models is an indication that some X-ray sources are optically thick thermal emitters.

The spectra of the remaining four sources were fitted poorly by all three models. In three of these cases the models clearly were inadequate to explain the data, and we conclude that either the sources are confused or more complex emission processes are at work.

We would like to acknowledge support of the staffs of the Sounding Rocket Branch of Goddard Space Flight Center and of the Comissao Nacional de Atividades Espaciais of Brazil. This work was supported by the National Aeronautics and Space Administration under Grant NGR 05-003-278.

REFERENCES

Bowyer, C. S., Lampton, M., Mack, J. E., and de Mendonca, F. 1970, *Ap. J. (Letters)*, 161, L1.

Bradt, H., Burnett, B., Mayer, W., Rappaport, S., and Schnopper, H. 1971, *Nature*, 229, 96.

Bradt, H., Naranan, S., Rappaport, S., and Spada, G. 1968, *Ap. J.*, 152, 1005.

Brown, R. L., and Gould, R. J. 1970, *Phys. Rev.*, D1, 2252.

Chodil, G., Mark, H., Rodrigues, R., Seward, F., Swift, C. D., Hiltner, W. A., Wallerstein, G., and Mannery, E. 1967, *Phys. Rev. (Letters)*, 19, 681.

Cooke, B. A., and Pounds, K. A., *Nature, Phys. Sci.* 229, 144, 1971.

Cooke, B. A., Pounds, K. A., Stewardson, E. A., and Adams, D. J. 1967, *Ap. J. (Letters)*, 150, L189.

Evans, R. D. 1955, *The Atomic Nucleus*, (New York: McGraw-Hill), p. 775.

Fisher, P. C., Jordan, W. C., Meyerott, A. J., Acton, L. W., and Rothig, D. T. 1967, *Ap. J.*, 147, 1209.

Friedman, H., Byram, E. T., and Chubb, T. A. 1967, *Science*, 156, 374.

Giacconi, R., Kellogg, E., Gorenstein, P., Gursky, H., and Tananbaum, H. 1971, *Ap. J. (Letters)*, 165, L27.

Gorenstein, P., Giacconi, R., and Gursky, H. 1967, *Ap. J. (Letters)*, 150, L85.

Greene, J. 1959, *Ap. J.* 130, 693.

Gursky, H., Gorenstein, P., and Giacconi, R. 1967, *Ap. J. (Letters)*, 150, L75.

Harries, J., McCracken, K. G., Francey, R. J., and Fenton, A. G. 1967, *Nature*, 215, 38.

Lampton, M., Bowyer, C. S., and Harrington, S. 1970, *Ap. J.*, **162**, 181.

Lampton, M., Bowyer, S., Mack, J. E., and Margon, B. 1971, *Ap. J. (Letters)*, **168**, L1.

Lewin, W. H. G., Clark, G. W., Gerassimenko, M., and Smith, W. B. 1969, *Nature*, **223**, 1142.

Lewin, W. H. G., Ricker, G. R., and McClintock, J. E. 1971, *Ap. J. (Letters)*, **169**, L17.

MacGregor, A., Seward, F., and Turiel, I. 1969, *Ap. J.*, **161**, 979.

Margon, B., Bowyer, S., Lampton, M., and Cruddace, R. 1971b, *Ap. J. (Letters)*, **169**, L45.

Margon, B., Lampton, M., Bowyer, S., and Cruddace, R. 1971a, *Ap. J. (Letters)*, **169**, L23.

Mayer, W., Bradt, H. V., and Rappaport, S. 1970, *Ap. J. (Letters)*, **159**, L115.

Rao, U. R., Chitnis, E. V., Sharma, D. P., Prakasarao, A. S., and Jayanthi, U. B. 1971, *Nature*, **229**, 248.

Rappaport, S., Bradt, H. V., Naranan, S., and Spada, G. 1969, *Nature*, **221**, 428.

Seward, F. D. 1970, Lawrence Radiation Laboratory, Livermore, University of California, Report UCID-15622.

Tananbaum, H., Gursky, H., Kellogg, E., and Giacconi, R. 1971, *Ap. J. (Letters)*, **168**, L25.

TABLE 1

CODE IDENTIFYING RESEARCH GROUPS AND ASSOCIATED FLIGHT DATES

Code	Research group	Flight date		Reference
NRL I	Naval Research Laboratory	1964	June 16	*Science*, 156, 374, 1967
NRL II	Naval Research Laboratory	1965	April 25	*Science*, 156, 374, 1967
LMSC	Lockheed Missiles and Space Company	1965	Sept. 30	*Ap. J.*, 147, 1209, 1967
ASE	American Science and Engineering	1966	Oct. 11	*Ap. J.*, 150, L75, 1967 *Ap. J.*, 150, L85, 1967
LRL I	Lawrence Radiation Laboratory, Livermore	1967	May 18	*Phys. Rev. Lett.*, 19, 681, 1967
MIT I	Massachusetts Institute of Technology	1967	July 7	*Ap. J.*, 152, 1005, 1968 *Nature*, 221, 428, 1969
UL I	University of Leicester	1968	June 12	Preprint, 1971
MIT II	Massachusetts Institute of Technology	1968	July 26	*Ap. J.*, 159, L115, 1970
LRL II	Lawrence Radiation Laboratory, Livermore	1968	Nov. 3	*Ap. J.*, 161, 979, 1969
UL II	University of Leicester	1969	April 1	*Nature Phys. Sci.* 229 144, 1971
UCB	University of California, Berkeley	1969	June 14	This paper
MIT III	Massachusetts Institute of Technology	1969	Oct. 2	*Nature*, 229, 96, 1971
PRL	Physical Research Laboratory, India	1969	Dec. 7	*Nature*, 229, 248, 1971
UHURU	American Science and Engineering	1970 1971	Dec. 27 April 25	*Ap. J.*, 165, L27, 1971 *Ap. J.*, 168, L25, 1971

TABLE 2

NEW POSITIONS OF GALACTIC X-RAY SOURCES IN THE SOUTHERN HEMISPHERE SKY

ℓ°_{II}	b°_{II}	UCB designation	Possible identifications with sources in Seward's catalogue (1970)	Possible identifications with sources seen by UHURU
336.8 ± 0.5	0 ± 0.5	GX 337+0	---	J1
326.6 ± 0.5	4.5 ± 1.5	GX 327+4.5	Lup 1	H1
321.4 ± 0.5	-0.5 ± 1.5	GX 321-0.5	Nor 2	G1
357 ± 0.5	2.5 ± 0.5	GX 357+2.5	---	O1

TABLE 3

SUMMARY OF ENERGY FLUX MEASUREMENTS OF GALACTIC X-RAY SOURCES

Source	Flux from the source between 1 and 10 keV* (10^{-8} ergs/cm^2 sec)							
	NRL I 1964	NRL II 1965	ASE 1966	MIT I 1967	LRL I 1967	MIT II 1968	LRL II 1968	UCB 1969
GX 321-0.5		0.5						1.6
GX 327+4.5		0.25			1.7			1.3
GX 337+0		1.0						0.8
GX 340+0		2.3				1.2		1.3
GX 340+6		0.8				1.3		0.8
GX 349+2	1.7	3.1	0.8			1.05	2.6	1.95
GX 357+2.5								0.30
GX 3+1				0.5		0.35		0.5
GX 5-1			1.1	1.4		1.85		1.65
GX 9+1		3.4	1.25	0.9		1.0		1.35
GX 13+1	1.8		0.4	0.4		0.6		1.1
GX 17+2		2.4	0.4	0.7	1.3	1.35		1.1

* Each column is identified by the code given in Table 1 and the date of the corresponding flight.

TABLE 4

BEST FITTING SPECTRA OF GALACTIC X-RAY SOURCES

	Black body model				Bremsstrahlung model				Power law model			
	T	N_H	Confidence	C	T	N_H	Confidence	C	n	N_H	Confidence	C
SOURCE	10^7°K	10^{22}H/cm^2	%	(eq. 3)	10^7°K	10^{22}H/cm^2	%	(eq. 1)		10^{22}H/cm^2	%	(eq. 2)
GX 321-0.5	1.1	0.79	33	2.33	3.55	2.5	18	17.05	2.93	3.5	0.2	29.0
GX 327+.5	1.25	0	0.2	0.90	7.1	0.79	76	21.0	2.10	1.1	30	75.1
GX 337+0	1.6	1.0	0.03	0.285	3.55	7.1	0.05	14.0	3.35	10.0	0.005	50.1
GX 340+0	1.55	1.2	25	0.45	7.1	4.0	8.3	8.3	2.25	5.0	3.8	10.20
GX 340+6*	1.2	0.13	0.8	0.61	12.5	0.35	10.6	3.16	1.70	0.50	7.8	2.10
GX 349+2	1.25	0.1	10^{-6}	1.36	10.0	1.1	0.00015	7.34	1.80	1.3	$<10^{-6}$	5.19
GX 357+2.5	1.0	1.0	3.8	0.634	5.6	0.35	24	1.33	2.10	0.56	24	1.08
GX 3+1	1.0	0.79	0.12	1.11	2.8	2.5	0.01	7.76	3.15	3.5	0.003	18.9
GX 9+1	1.25	0.25	28	1.00	5.6	1.6	21	8.44	2.20	2.0	15	7.91
GX 17+2	0.95	1.6	4.2	3.94	2.5	3.5	0.5	24.3	3.55	5.0	0.1	59.2

* Confused slightly with a weaker source, Sco XR-7.

TABLE 5

GALACTIC X-RAY SOURCES EXHIBITING SPECTRAL VARIABILITY

Source	Temperature of best Bremsstrahlung spectrum* (10^7 °K)							Hydrogen density in line-of-sight* ($10^{22}/cm^2$)			
	LMSC 1965	ASE 1966	MIT I 1967	UL I 1968	UCB 1969	PRL 1969	UHURU 1970	ASE 1966	MIT I 1967	UCB 1969	UHURU 1970
GX 321-0.5				13	3.55	6.0				2.5	
GX 349+2	16	3.1			10			3.2		1.1	
GX 9+1	7	4.3	>9		5.6			3.2	<0.7	1.6	
GX 17+2	9	5.1			2.5		5-15.5	3.2		3.55	2.5

* Each column is identified by the code given in Table 1 and the date of the corresponding flight.

Figure Captions

Fig. 1. The track of the center of the collimator fields of view and the galactic X-ray sources observed during the flight. The black error boxes represent new or improved source positions obtained from this flight. The solid error circles are the results of the MIT surveys of galactic sources (Bradt *et al.* 1971), and the dashed circles and boxes are sources listed in the LRL catalogue (Seward, 1970) which were not identified positively in our results, but which may be related to the sources we observed.

Fig. 2. The measured spectrum of GX 321-0.5, the best-fitting black body spectrum, and spectra measured by other groups. The contours in the lower graph enclose spectral parameters for which the fitting confidences are within $e^{-\frac{1}{2}}$ of the peak confidence. The point of peak confidence is represented by a triangle for the black body, a circle for the bremsstrahlung, and a cross for the power-law case. The power-law contour does not appear in this figure, as we show contours only where the best fit is satisfactory, i.e., the peak confidence lies between 10 and 90%.

Fig. 3. The measured spectrum of GX 327+4.5, the best-fitting bremsstrahlung spectrum, and the spectrum measured in 1967 by LRL.

Fig. 4. The measured spectrum of GX 337+0 and the best-fitting bremsstrahlung spectrum. No tolerance contours are shown in this and subsequent figures, where a satisfactory fit was not obtained with any model. An absence of other results in this and some of the subsequent

figures of other results indicates that we have been unable to find published measurements of the source spectrum.

Fig. 5. The measured spectrum of GX 340+0 and the best-fitting black body spectrum.

Fig. 6. The measured spectrum of GX 340+6 and the best-fitting bremsstrahlung spectrum.

Fig. 7. The measured spectrum of GX 349+2, the best fitting bremsstrahlung spectrum, and the spectra measured by other groups. In the interest of clarity, only four of the LMSC experimental points have been drawn.

Fig. 8. The measured spectrum of GX 357+2.5 and the best-fitting bremsstrahlung spectrum.

Fig. 9. The measured spectrum of GX 3+1 and the best-fitting black body spectrum.

Fig. 10. The measured spectrum of GX 9+1, the best-fitting black body spectrum, and the spectra measured by other groups. In the interest of clarity, only three of the LMSC experimental points have been drawn.

Fig. 11. The measured spectrum of GX 17+2, the best-fitting black body spectrum, and the spectra measured by other groups. In the interest of clarity, only four the the LMSC experimental points have been drawn.

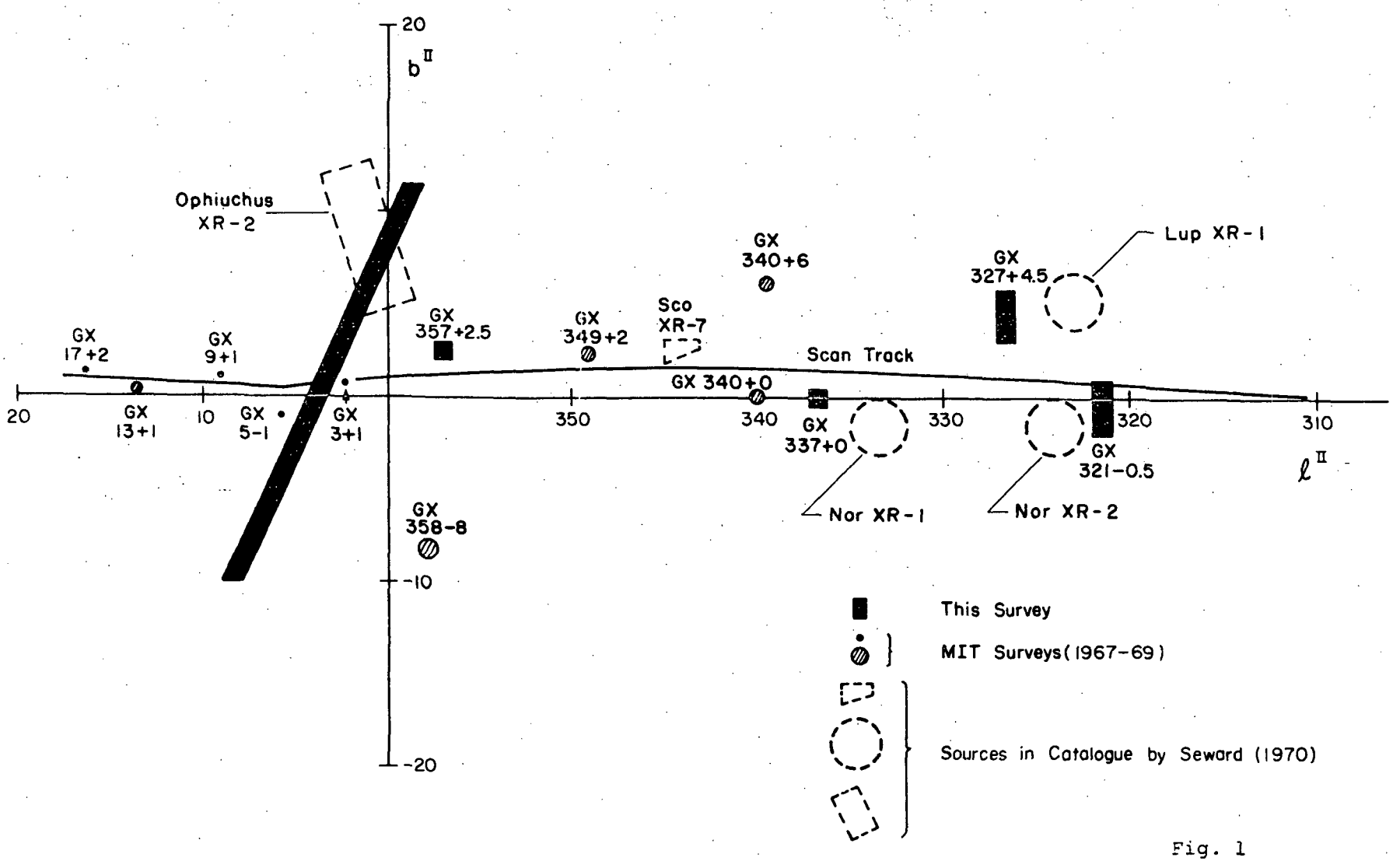
20
b^{II}
Ophiuchus
XR-2
GX
17+2
GX
9+1
GX
13+1
GX
5-1
GX
3+1
GX
357+2.5
GX
349+2
Sco
XR-7
GX
340+6
Scan Track
GX 340+0
GX
337+0
GX
327+4.5
Lup XR-1
GX
321-0.5
Nor XR-1
Nor XR-2
GX
358-8
20
10
350
340
330
320
310
ℓ^{II}
-10
-20
This Survey
MIT Surveys(1967-69)
Sources in Catalogue by Seward (1970)

Fig. 1

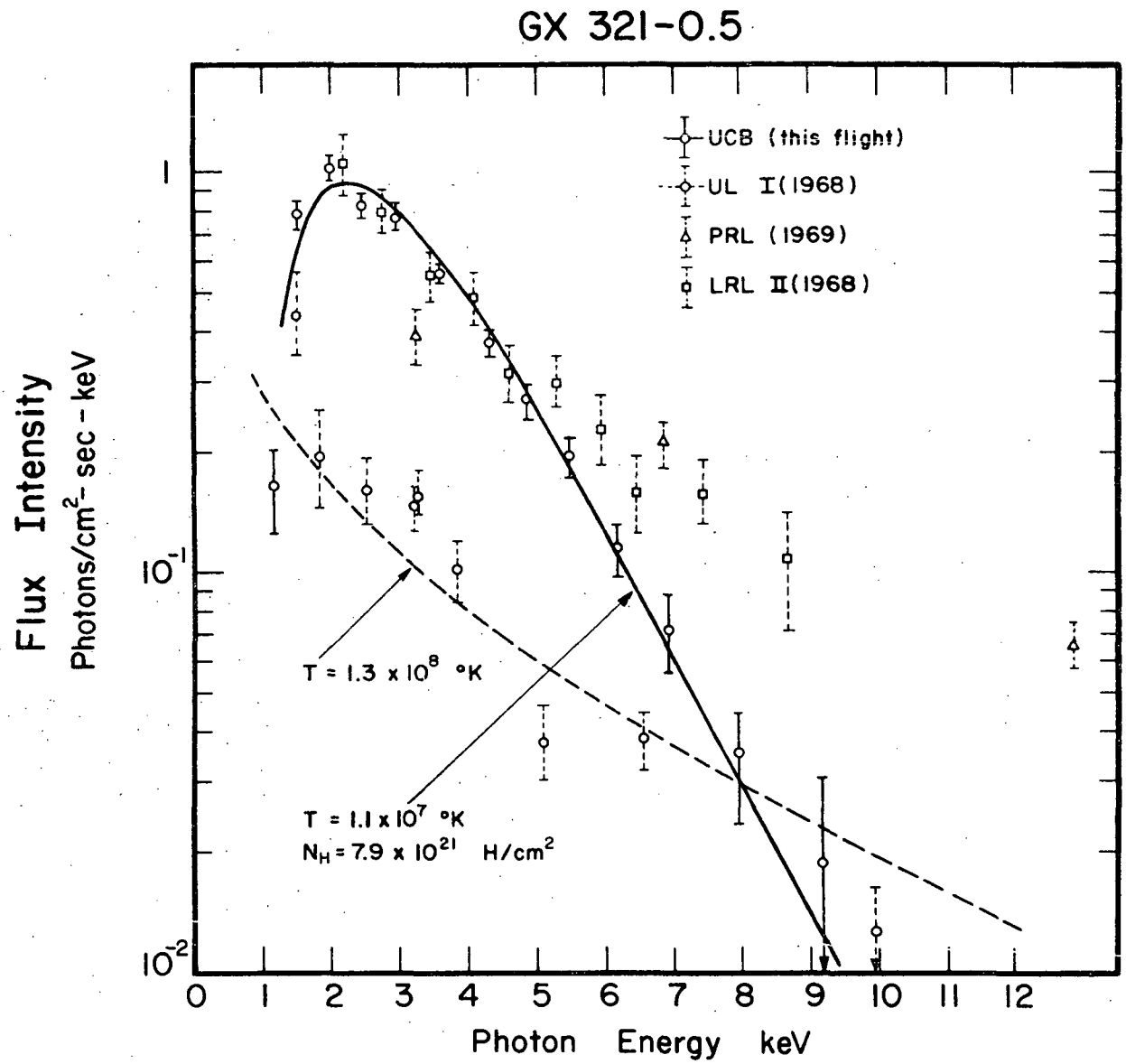
GX 321-0.5
UCB (this flight)
UL I(1968)
PRL (1969)
LRL II(1968)
Flux Intensity
Photons/cm²- sec - keV
1
10⁻¹
10⁻²
T = 1.3 x 10⁸ °K
T = 1.1 x 10⁷ °K
N_H = 7.9 x 10²¹ H/cm²
0 1 2 3 4 5 6 7 8 9 10 11 12
Photon Energy keV

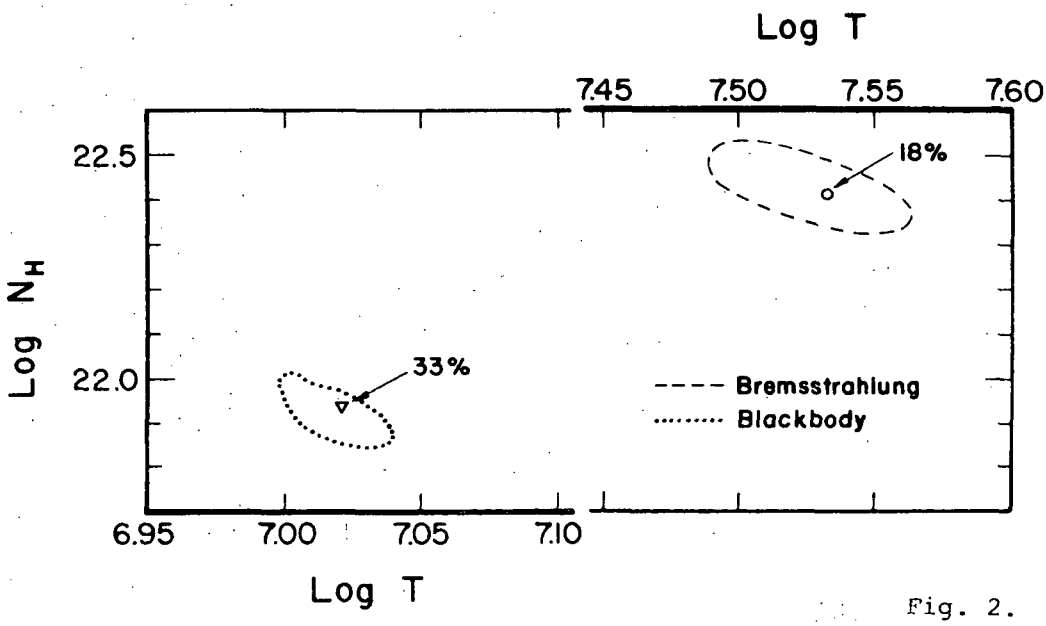
Log T
7.45 7.50 7.55 7.60
22.5
22.0
Log N_H
18%
33%
Bremsstrahlung
Blackbody
6.95 7.00 7.05 7.10
Log T

Fig. 2.

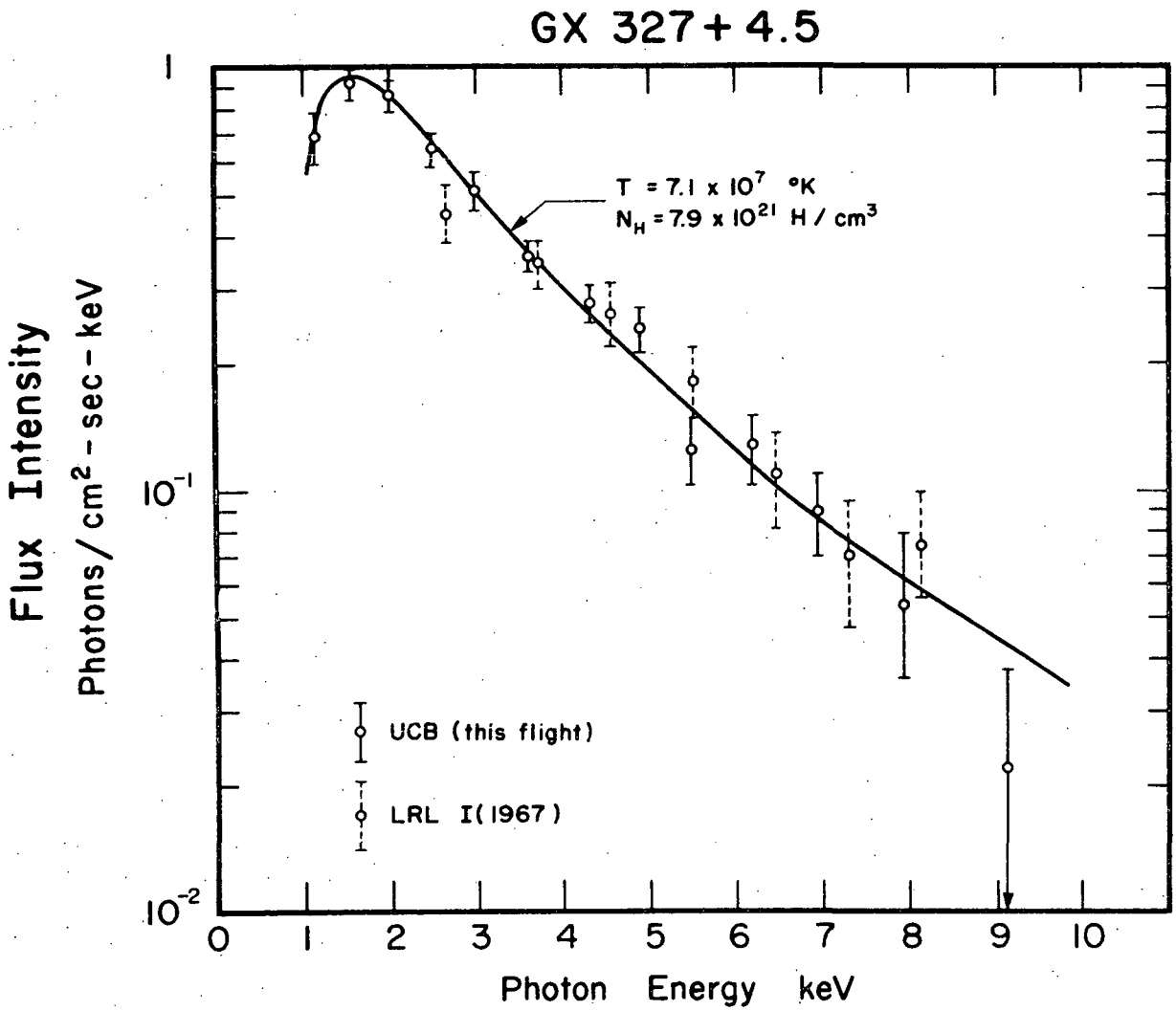
GX 327+4.5
T = 7.1 x 10^7 °K
N_H = 7.9 x 10^21 H / cm^3
UCB (this flight)
LRL I(1967)
Flux Intensity
Photons / cm^2 - sec - keV
Photon Energy keV

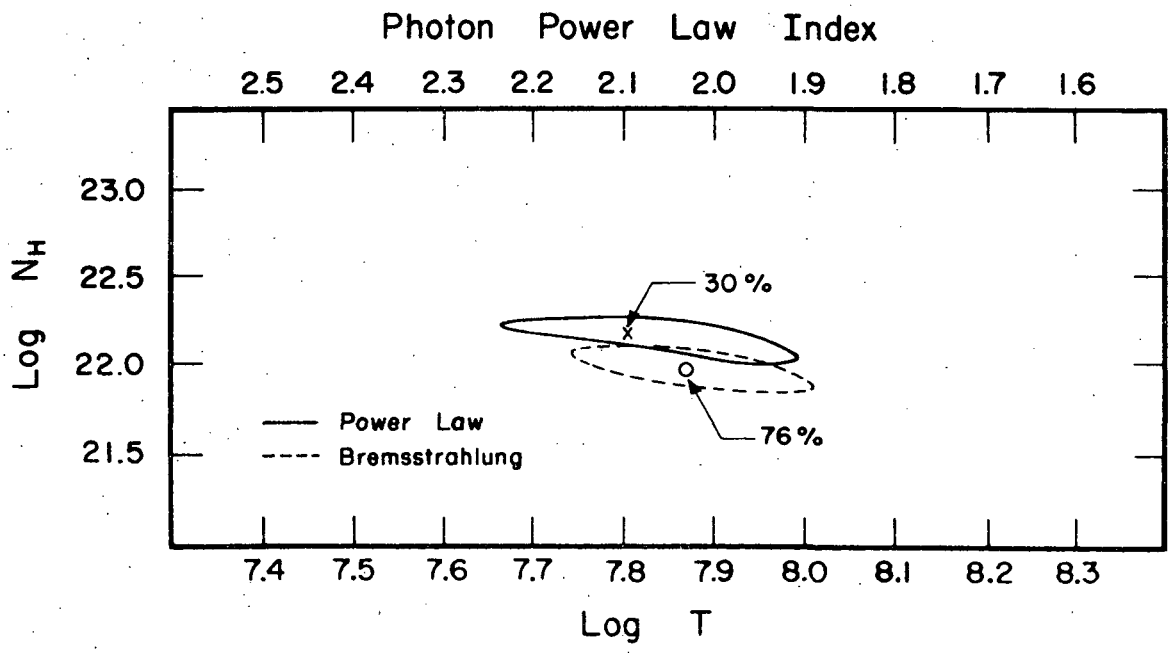
Photon Power Law Index
30 %
76 %
Power Law
Bremsstrahlung
Log N_H
Log T

Fig. 3.

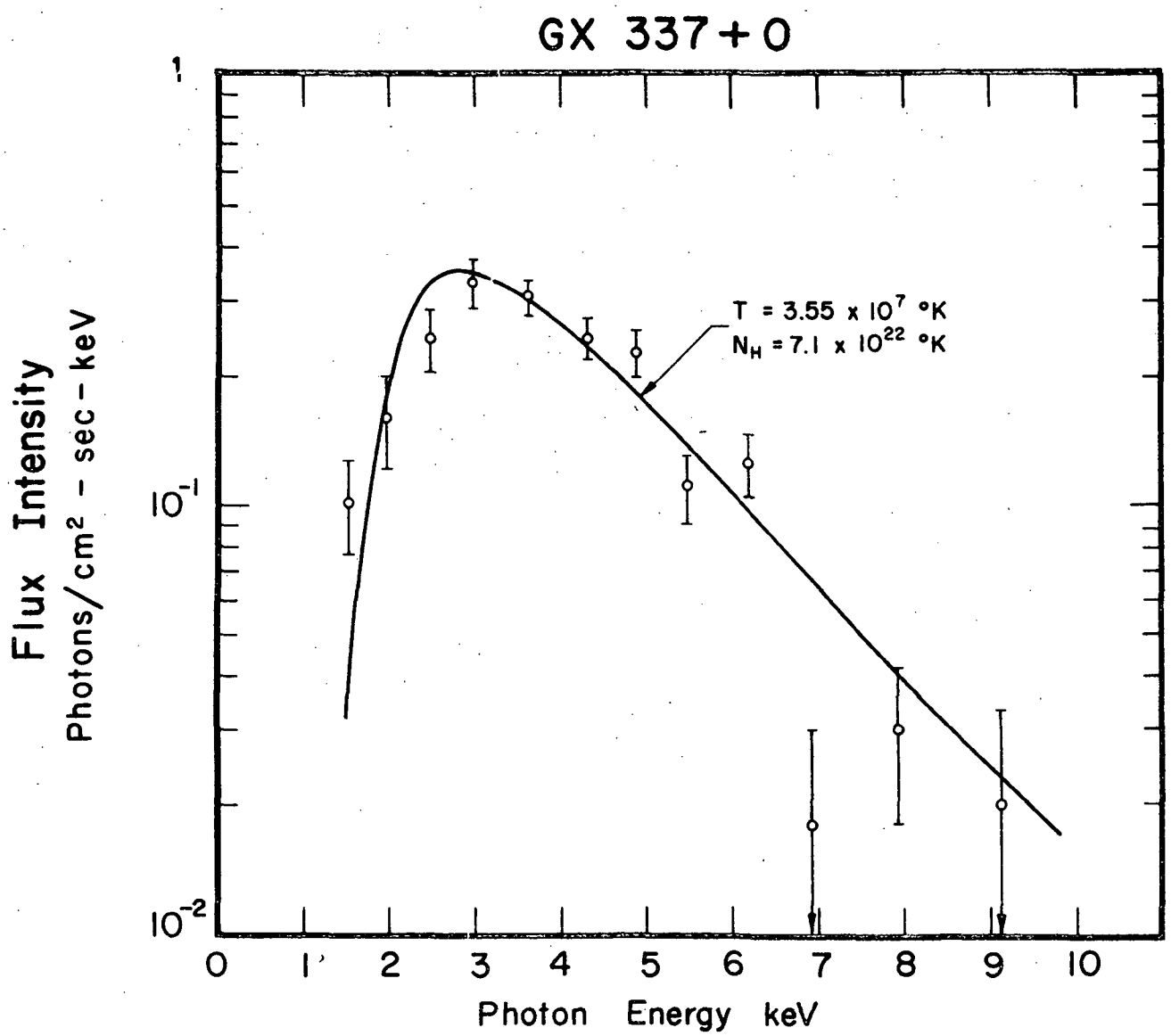
GX 337+0
Flux Intensity
Photons/cm² - sec - keV
1
10⁻¹
10⁻²
0
1
2
3
4
5
6
7
8
9
10
Photon Energy keV
T = 3.55 x 10⁷ °K
N_H = 7.1 x 10²² °K

Fig. 4.

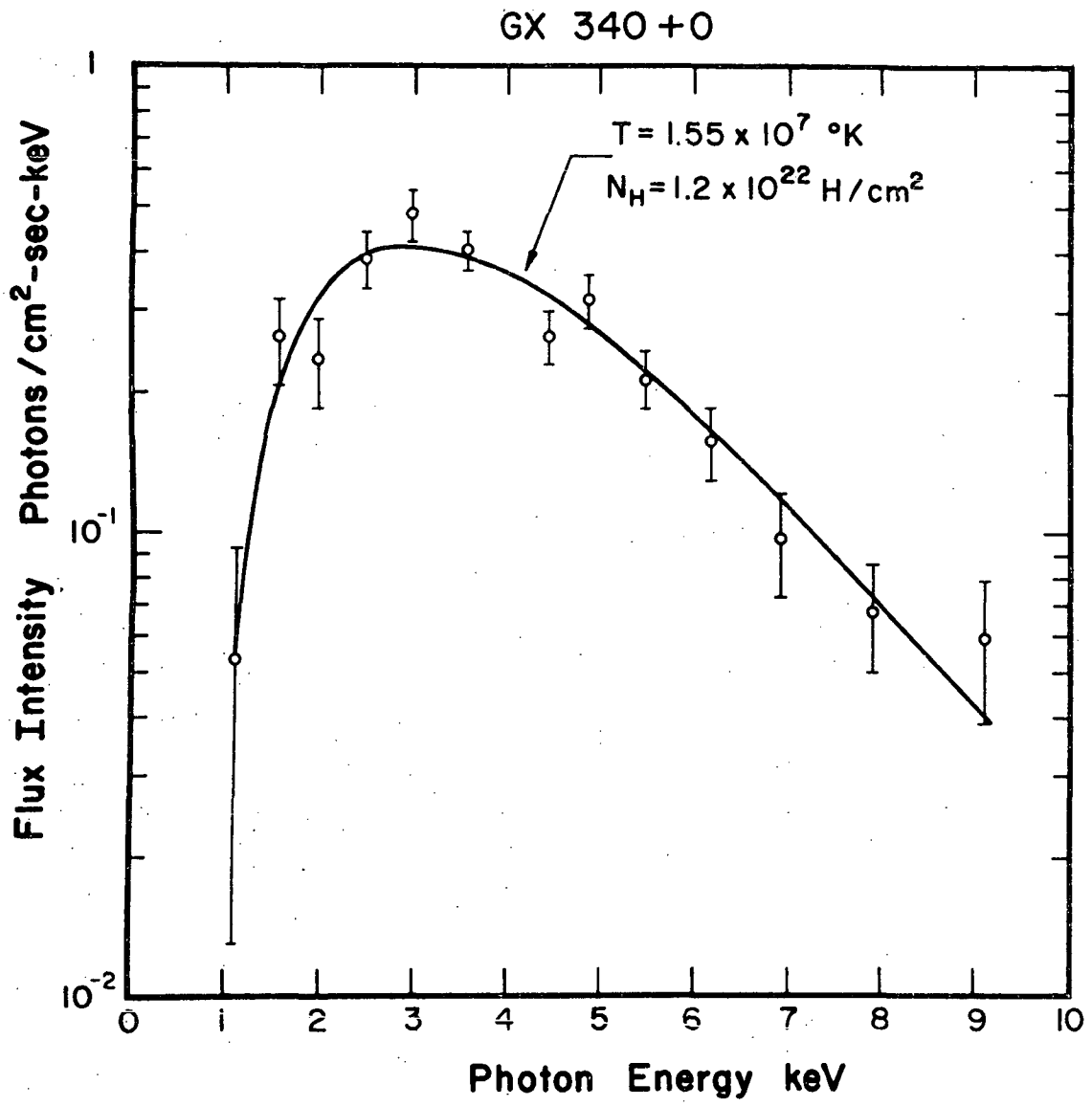
GX 340+0
T = 1.55 x 10^7 °K
N_H = 1.2 x 10^22 H/cm^2
Flux Intensity Photons/cm^2-sec-keV
1
10^-1
10^-2
0
1
2
3
4
5
6
7
8
9
10
Photon Energy keV

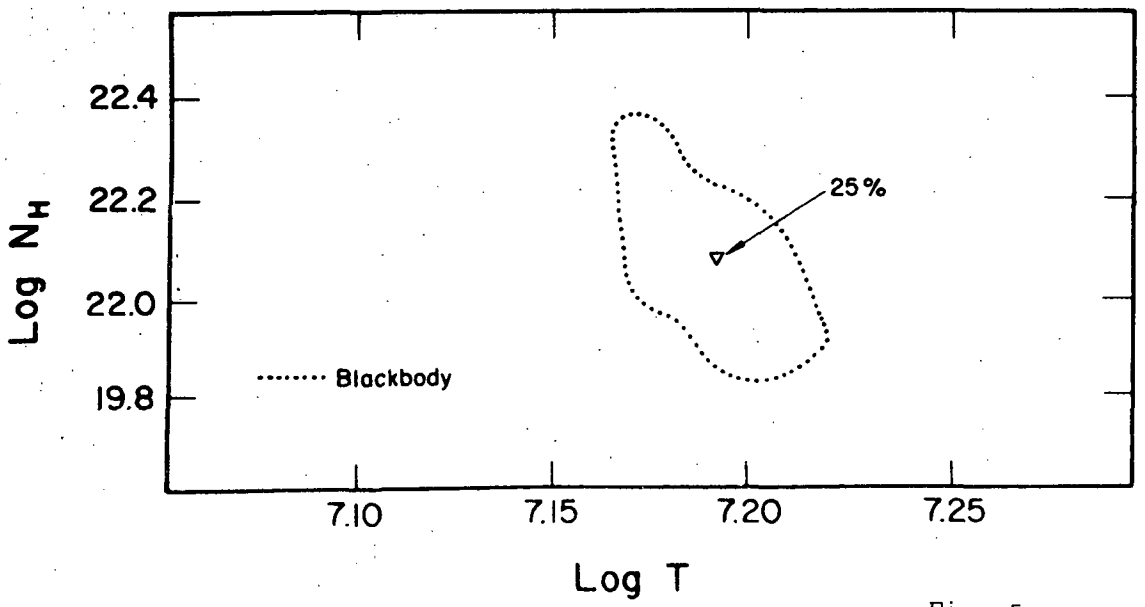
Log N_H
22.4
22.2
22.0
19.8
25%
Blackbody
7.10
7.15
7.20
7.25
Log T

Fig. 5.

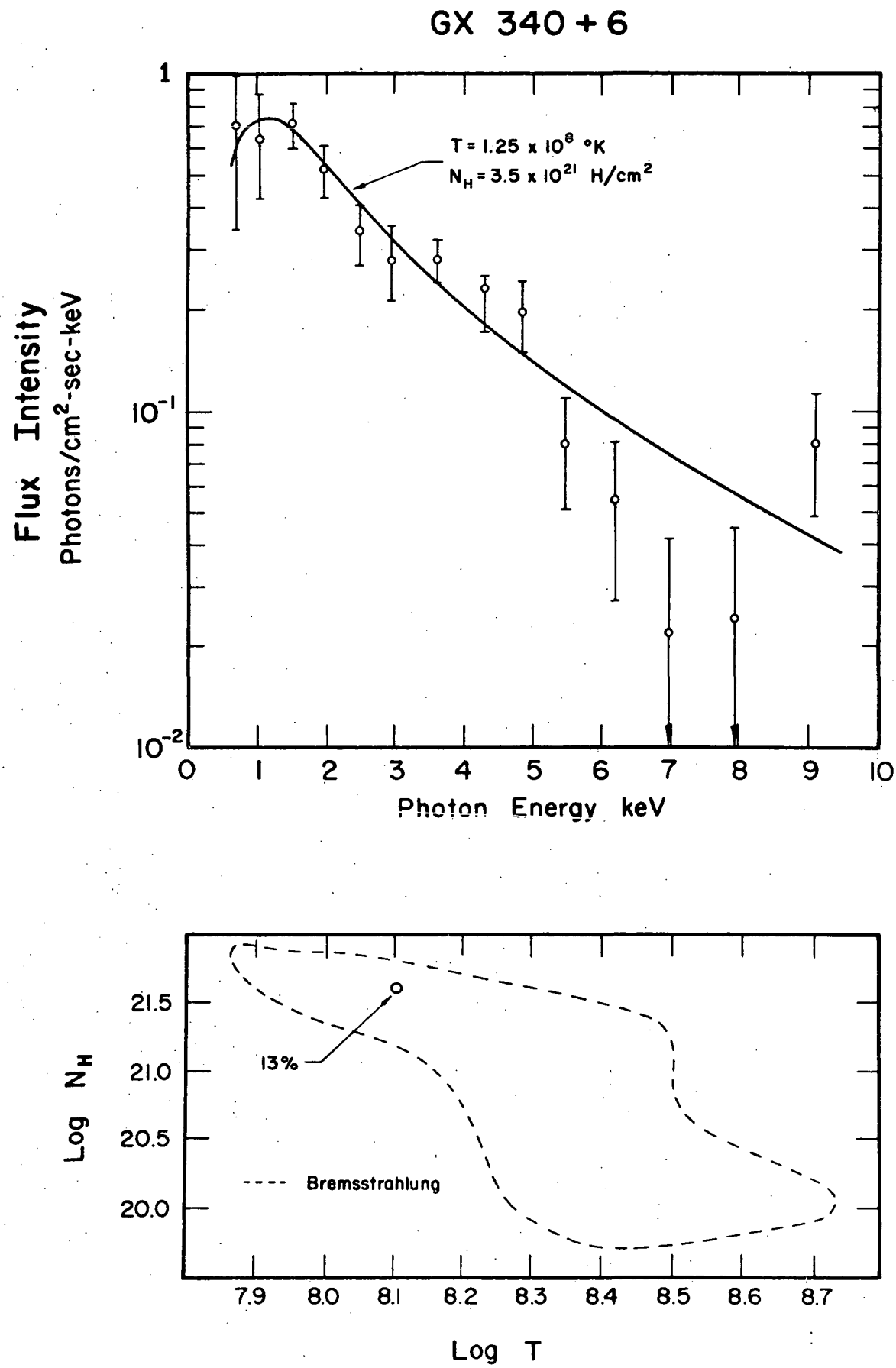
GX 340 + 6
T = 1.25 x 10^8 °K
N_H = 3.5 x 10^21 H/cm^2
Flux Intensity
Photons/cm^2-sec-keV
1
10^-1
10^-2
0 1 2 3 4 5 6 7 8 9 10
Photon Energy keV
13%
Bremsstrahlung
Log N_H
21.5
21.0
20.5
20.0
7.9 8.0 8.1 8.2 8.3 8.4 8.5 8.6 8.7
Log T

Fig. 6.

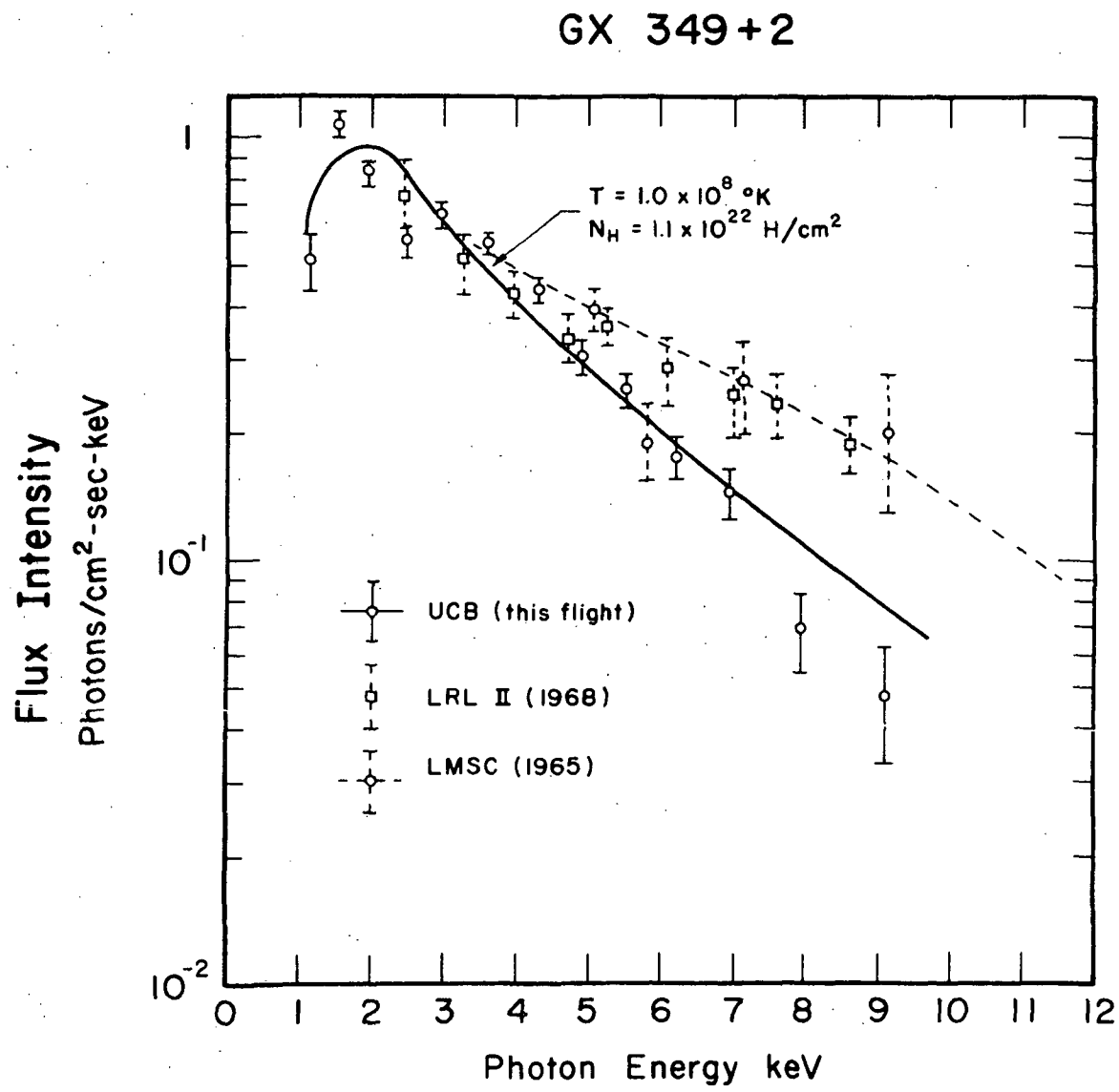
GX 349+2
T = 1.0 x 10^8 °K
N_H = 1.1 x 10^22 H/cm^2
UCB (this flight)
LRL II (1968)
LMSC (1965)
Flux Intensity
Photons/cm^2-sec-keV
Photon Energy keV
1
10^-1
10^-2
0
1
2
3
4
5
6
7
8
9
10
11
12

Fig. 7.

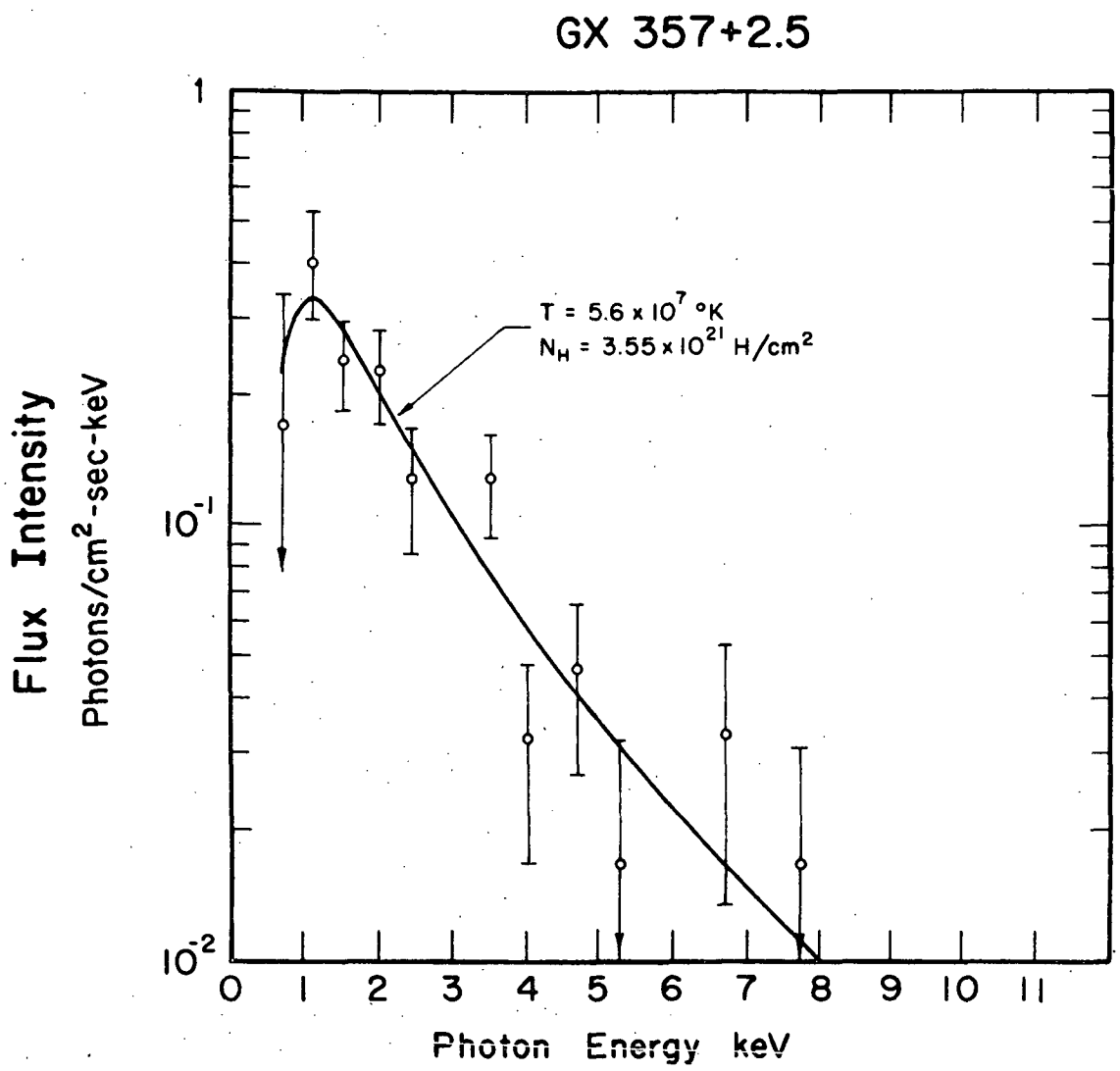
GX 357+2.5
Flux Intensity
Photons/cm²-sec-keV
1
10⁻¹
10⁻²
T = 5.6 x 10⁷ °K
N_H = 3.55 x 10²¹ H/cm²
0 1 2 3 4 5 6 7 8 9 10 11
Photon Energy keV

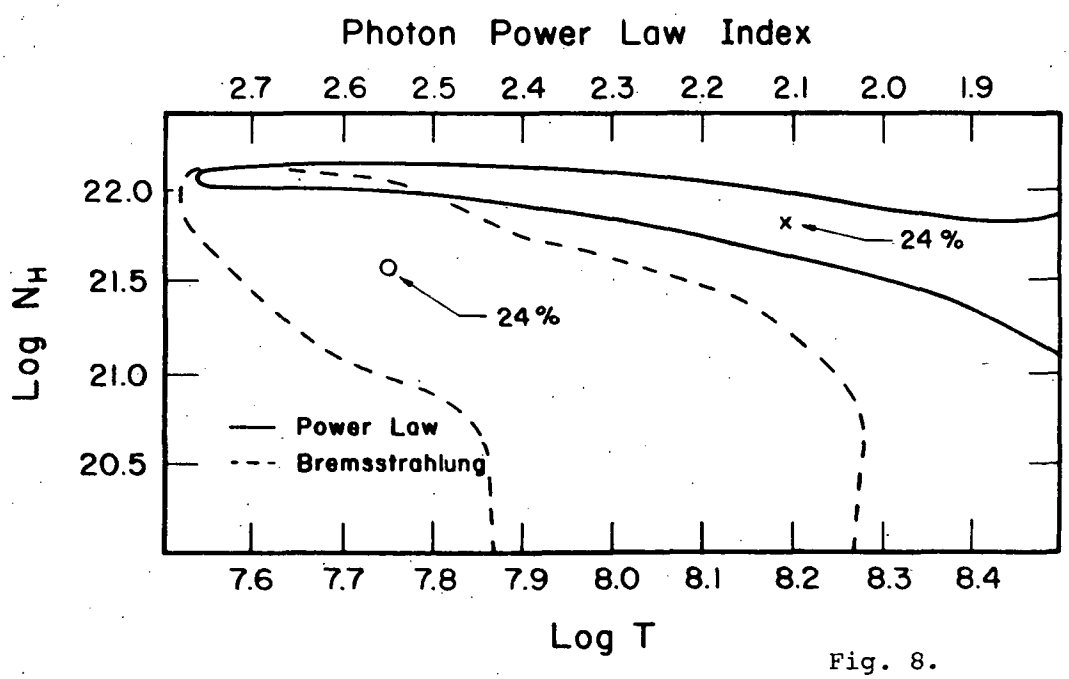
Photon Power Law Index
2.7 2.6 2.5 2.4 2.3 2.2 2.1 2.0 1.9
Log N_H
22.0
21.5
21.0
20.5
24 %
24 %
Power Law
Bremsstrahlung
7.6 7.7 7.8 7.9 8.0 8.1 8.2 8.3 8.4
Log T

Fig. 8.

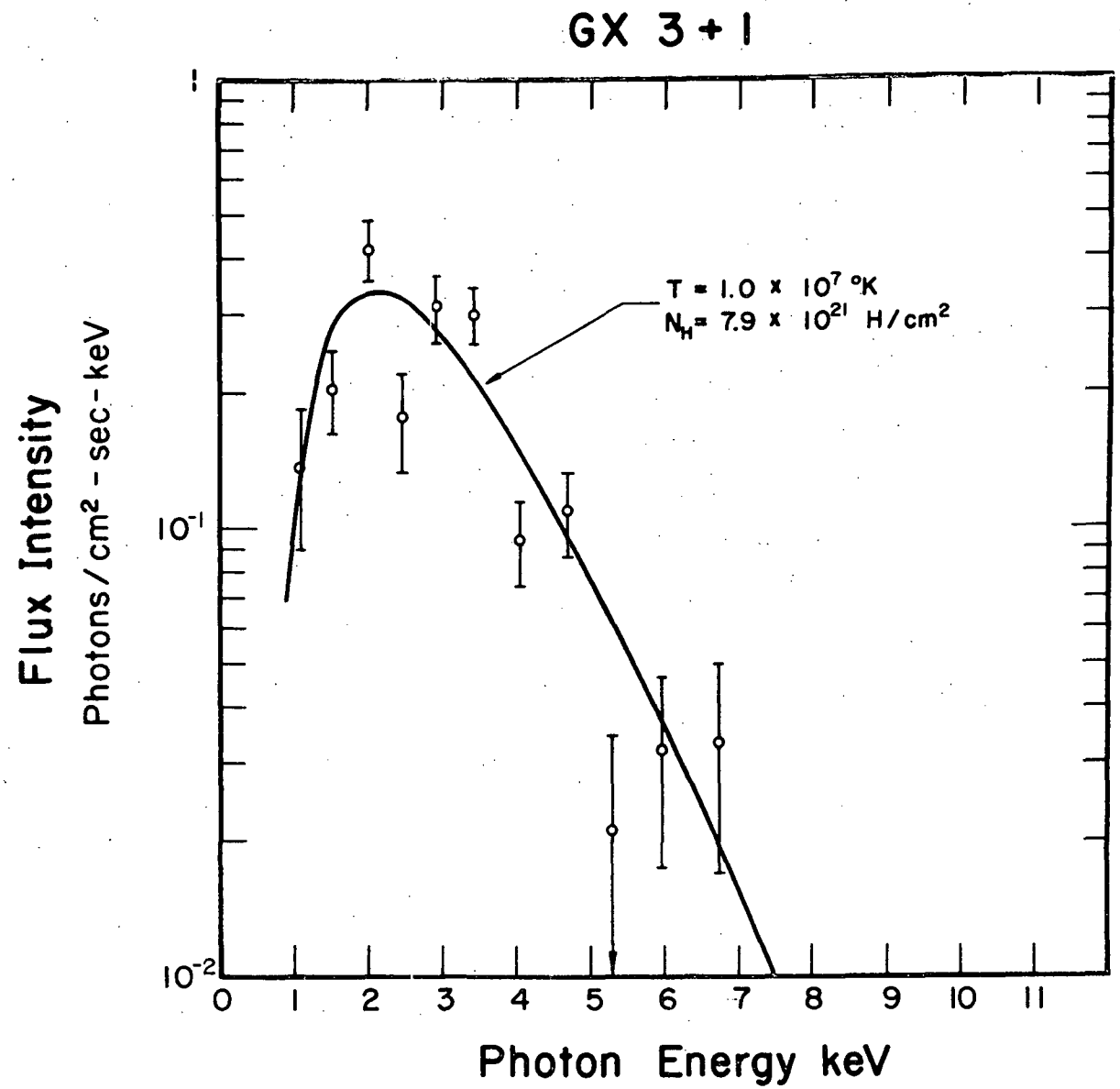
GX 3+1
T = 1.0 x 10^7 °K
N_H = 7.9 x 10^21 H/cm^2
Flux Intensity
Photons/cm^2 - sec - keV
1
10^-1
10^-2
0
1
2
3
4
5
6
7
8
9
10
11
Photon Energy keV

Fig. 9.

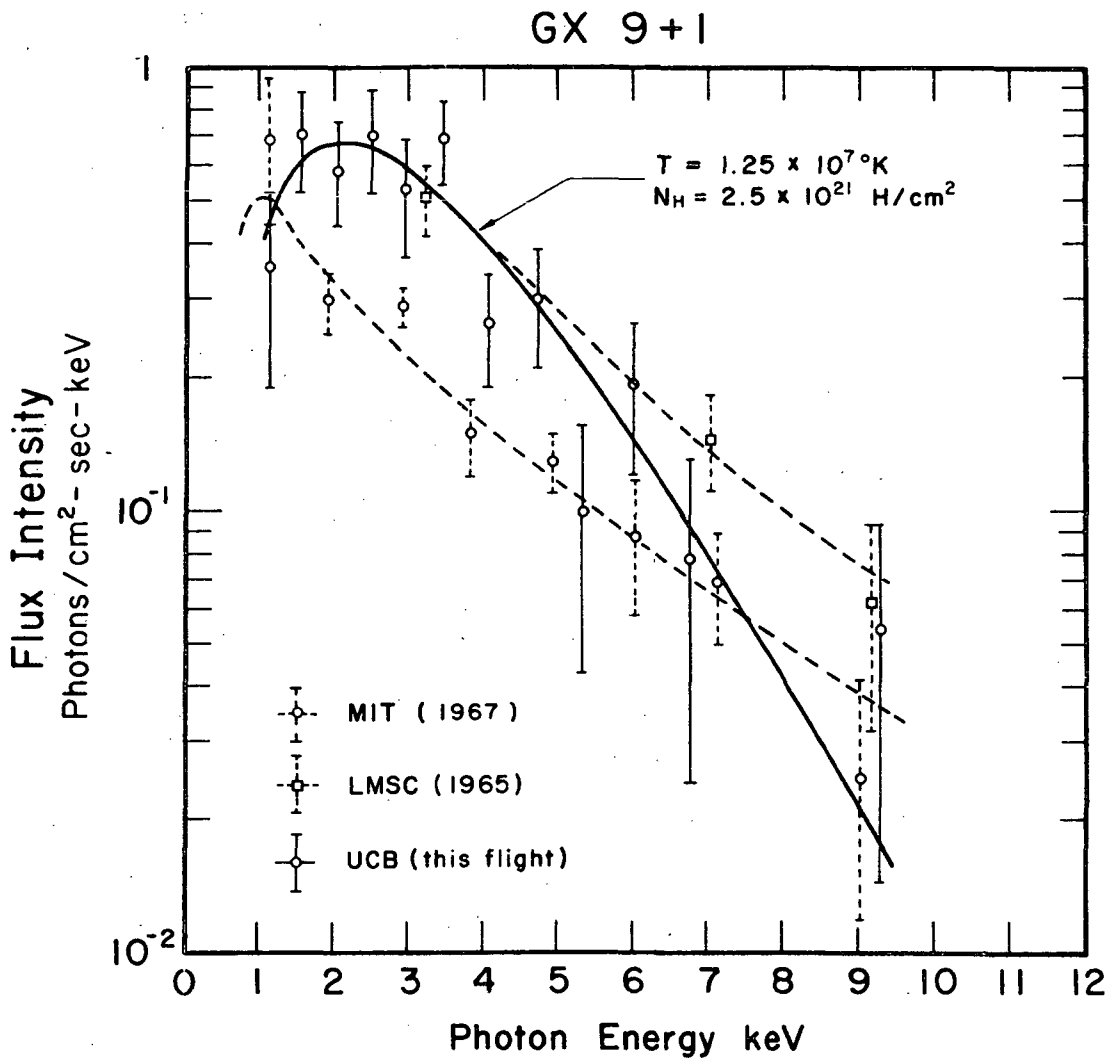
GX 9+1
T = 1.25 x 10^7 °K
N_H = 2.5 x 10^21 H/cm^2
Flux Intensity
Photons/cm^2-sec-keV
MIT (1967)
LMSC (1965)
UCB (this flight)
Photon Energy keV

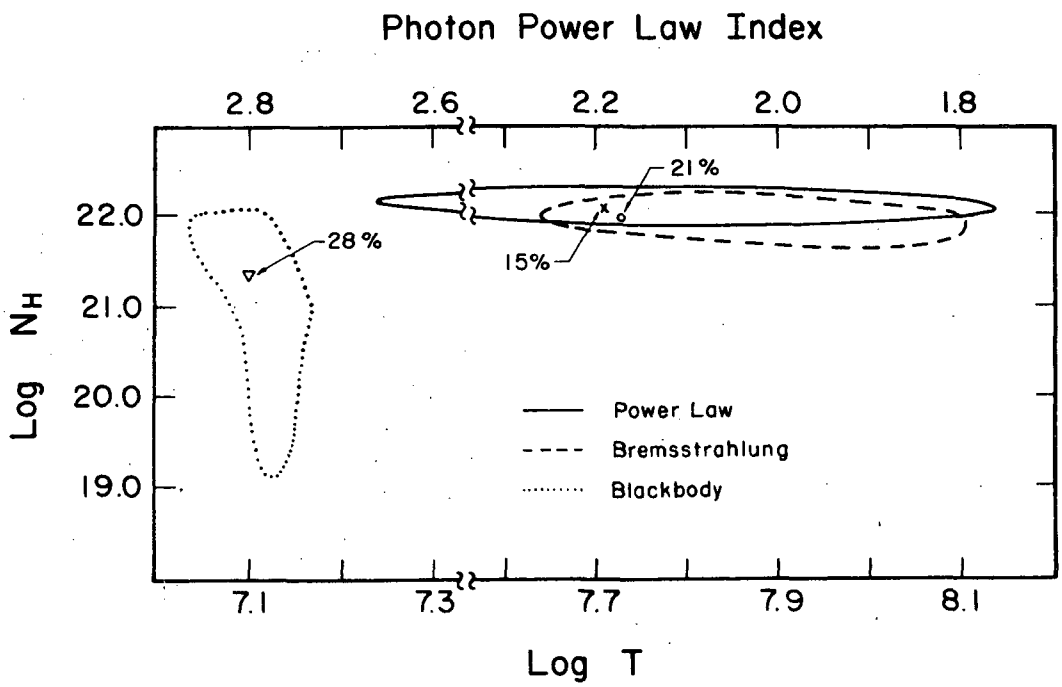
Photon Power Law Index
21%
28%
15%
Log N_H
Power Law
Bremsstrahlung
Blackbody
Log T

Fig. 10.

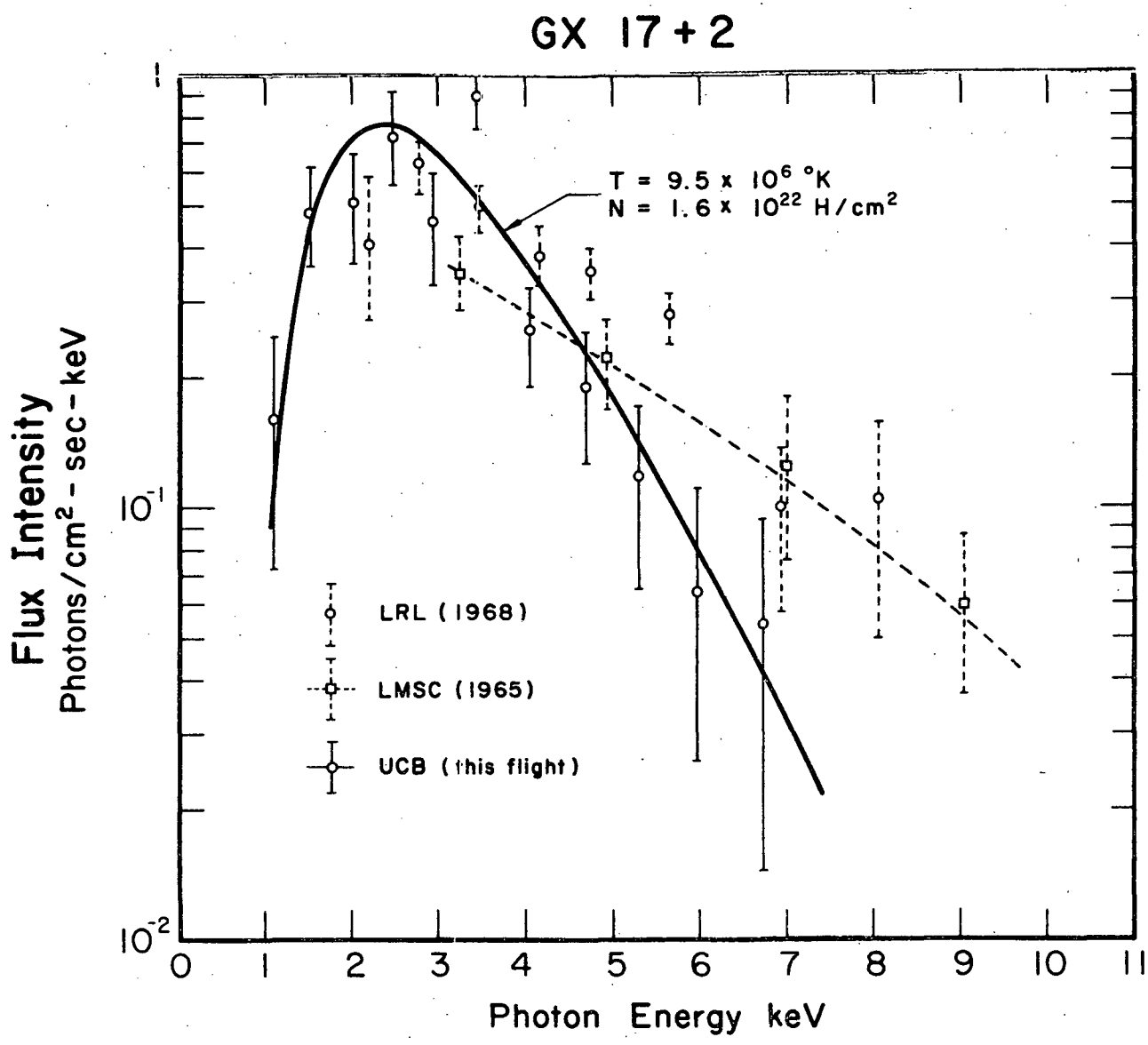
GX 17 + 2
T = 9.5 x 10^6 °K
N = 1.6 x 10^22 H/cm^2
LRL (1968)
LMSC (1965)
UCB (this flight)
Flux Intensity
Photons/cm^2 - sec - keV
10^-1
10^-2
0
1
2
3
4
5
6
7
8
9
10
11
Photon Energy keV

Fig. 11.